# Influence of Different Testing Methods on the Thermal Shock Resistance of Alumina Castable Samples

**Yaowu Wei, Christos G. Aneziris, Nan Li**

The thermal shock resistance of self-flow alumina based castables is investigated due to natural cooling, compressed air cooling and water cooling (quench) methods respectively. The residual *Young*'s modulus as well the residual bending strength are taken into account in order to compare the influence of different testing methods on the results. The pore size distribution, SEM analysis and computerized tomography are used to assist the study. The integrity of the sample is damaged dramatically by the application of water quenching test and does not reflect the real state of the thermal shock resistance of the castables in practice. The results based on compressed air cooling (quench) method are similar with that based on natural cooling process and are suitable to evaluate the thermal shock performance of the alumina castable samples.

## 1 Introduction

The evaluation on the thermal shock performance of refractories is still a very complex problem and the testing methods do not always meet the real application requirements. A number of papers are published in recent years dealing with the thermal shock resistance of different refractory materials as well as related testing methods [1–14].

The common used testing methods on thermal shock resistance of refractories can be listed in Tab. 1.

The most popular testing method on thermal shock resistance is based on application of heating-cooling cycles; the samples are heated under a certain temperature and then cooled (quench) in water or compressed air. The residual bending strength or residual Young's modulus of samples are used to evaluate the thermal shock resistance. The related equations are shown in the following.

$$R_b = \frac{B_1}{B_0} \times 100\% \quad (1)$$

$R_b$ is the residual bending strength of sample [%]

$B_1$ is the bending strength of sample after thermal shock [MPa]

$B_0$ is the bending strength of sample before thermal shock [MPa]

$$R_y = \frac{Y_1}{Y_0} \times 100\% \quad (2)$$

$R_y$ is the residual Young's modulus of sample [%]

$Y_1$ is the Young's modulus of sample after thermal shock [GPa]

$Y_0$ is the Young's modulus of sample before thermal shock [GPa]

**Tab. 1** Thermal shock resistance testing method for refractories [15]

| Thermal Shock Condition | Testing Method | Evaluation Basis |
|---|---|---|
| • heating or cooling<br>• heating-cooling cycles | • investigation on cracks<br>• weighting<br>• bending strength testing<br>• Young's modulus testing<br>• acoustic emission method | • crack condition checked by eyesight<br>• weight loss [%]<br>• residual bending strength [%]<br>• characteristic of acoustic emission during thermal shock |

Both residual bending strength and residual Young's modulus are useful to evaluate the thermal shock resistance of refractories, because bending strength and Young's modulus are very sensitive to the defects formed in the materials. Once the defects formed e.g. the length of crack exceeds critical value, the bending strength of the materials will decrease accordingly.

Compressed air quench or water quench method is widely used to test the thermal shock resistance of the refractories, but the paper deal with the influence of different testing method on the thermal shock resistance of refractories is rather less. This study

*Yaowu Wei, Nan Li*
*The Key State Laboratory Breeding Base of Refractories and Ceramics*
Wuhan University of Science and Technology,
430081 Wuhan
China

*Christos G. Aneziris*
*TU Bergakademie Freiberg*
Institute of Ceramic, Glass and Construction Materials
09569 Freiberg
Germany

Corresponding author: *Yaowu Wei*
E-mail: wywref@yahoo.com.cn

Keywords: thermal shock resistance, testing methods, alumina castables

Received: 05.02.2013
Accepted: 15.03.2013

**Tab. 2** Physical properties of the castables after sintering under 1600 °C

| Bending Strength [MPa] | Apparent Porosity [%] | Density [g/cm³] | Dynamic Young's Modulus $E_{\delta\psi v}$ [GPa] (Ultrasonic Impulse Technique) |
|---|---|---|---|
| 31,2 | 17,9 | 3,09 | 117,6 |

compares the results of thermal shock resistance of alumina based self-flow castables. These results were obtained by due different testing methods, including heating-natural air cooling cycles, heating-compressed air cooling cycles and heating-water cooling cycles. The results could be used as a reference for the further study and testing.

## 2 Experimental

The formulation of the castables is 89 % tabular alumina (*Almatis Corporation,* $Al_2O_3$ >99 %), 8 % active alumina and 3 % alphabond 300 (q = 0,25). The water content for the mixing is 5,7 % and the self-flowability value via flowcone test is 160 %.

$$F_S = \frac{D_{mean} - 100}{100} \times 100\% \qquad (3)$$

$F_s$ is self-flowability value of the castable;
$D_{mean}$ is mean value of the diameter of the castable;

The mixes are casted into 160 mm × 40 mm × 40 mm shapes, curing for 24 h and then demoulded, after that 24 h dried in air and additionally at 120 °C for 24 h. All samples are sintered at 1600 °C for 3 h. Finally, samples are thermal shocked by heating-nature air cooling, heating-compressed air cooling and heating-water cooling respectively.

The test pieces used in compressed air cooling test are heated up to 950 °C in an electric furnace and then removed, placed on a steel plate and exposed to blowing air for 5 min. Heating-cooling cycles are repeated for 1 to 5 frequencies. 45 samples were used for thermal shock resistance test. In case of water quench the samples are dried at 120 °C for 16 h after each shocked.

Bending strength of samples was determined at room temperature before and after thermal shock by the universal testing machine (*Toni-Processor B*/DE). The bending strength was calculated by using the following equation:

$$\sigma_f = \frac{3FL}{2bh^2} \qquad (4)$$

Where F is the maximum load, L is the span, b is the width of the samples and h is the thickness.

An ultrasonic testing machine instrument of transmission type (*STEINKAMP* ultrasonic tester BP-77/DE) was used. Through determining the ultrasonic velocity and bulk density of samples, it is possible to calculate the dynamic modulus of elasticity using the equation shown bellow:

$$E_{dyn} = \frac{(1+\mu_{dyn})*(1-2\mu_{dyn})}{(1-\mu_{dyn})}\rho\upsilon^2 \qquad (5)$$

Where $\upsilon$ is ultrasonic impulse velocity (m/s), $\rho$ is the density (kg/m³), $\mu_{dyn}$ is the dynamic *Poisson*'s ratio and 0,2 is appointed as the $\mu_{dyn}$ value here because 0,2 is common used for ceramic materials.

The SEM (*ESEM* XL30/NL) and pore size diffusion analysis (Pascal 140 und 440, *Porotec*) are used to investigate the microstructure change of samples, and the X-ray micro-computed tomography CT ALPHA (*Procon*/DE) assists the micro structure studies. X-ray microcomputed tomography is an efficient tool for analysis of refractory structures, and the application on the refractory structures is reported [16]. The geometrical structure of the shocked samples was investigated by 3D-image processing of X-ray tomography with the aid of an Alpha Computer Tomograph of Procon X-Ray (*Garbsen*/DE). This apparatus is equipped with two high power X-Ray guns 160 and 225 kV respectively as well as two different detectors (flat panel sensor with photodiode area of 120 mm × 120 mm and a digital X-ray detector with total area 410 mm × 410 mm). The measurement and the reconstruction will be performed using the software Voxel 6.0, whereas the visualization of the reconstructed volume data with the software VolumePlayerPlus (both developed at the *Fraunhofer Development Center* for X-ray technology). The maxima analysable sample is limited by the detector area and even more by the density of the material. The attainable spatial resolution is limited by the focal spot of the X-ray tube as well as by the size of detector pixels. Through special positioning of the sample between the X-ray gun and the detector voxel sizes of 5,9 µm could be realised for alumina samples 10 mm × 10 mm × 10 mm and 20 µm for alumina samples 25 mm × 25 mm × 25 mm. This is the edge length of the smallest detectable volume element within the sample.

## 3 Results and discussion

The physical properties of castables after sintering at 1600 °C are presented in Tab. 2.

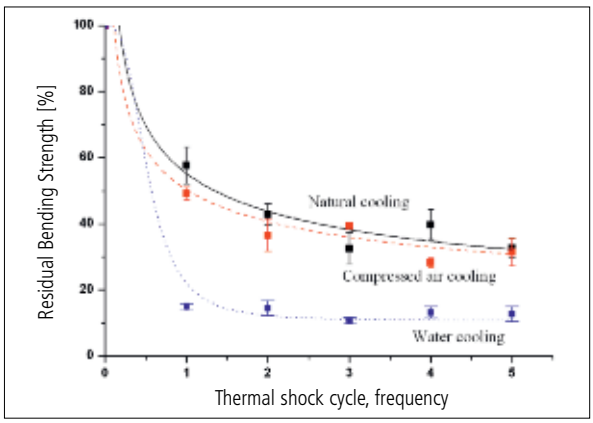


**Fig. 1** Residual bending strength of the samples

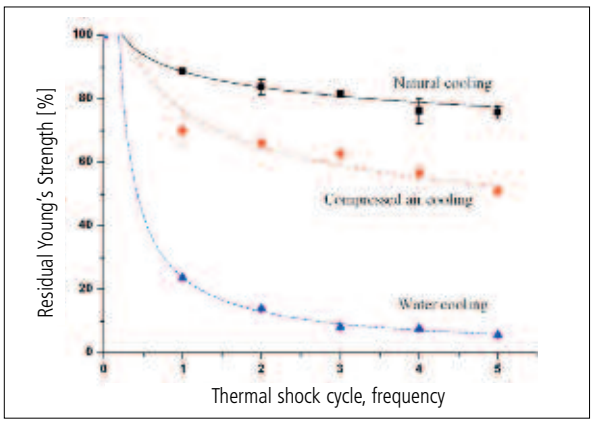


**Fig. 2** Residual Young's modulus of the samples

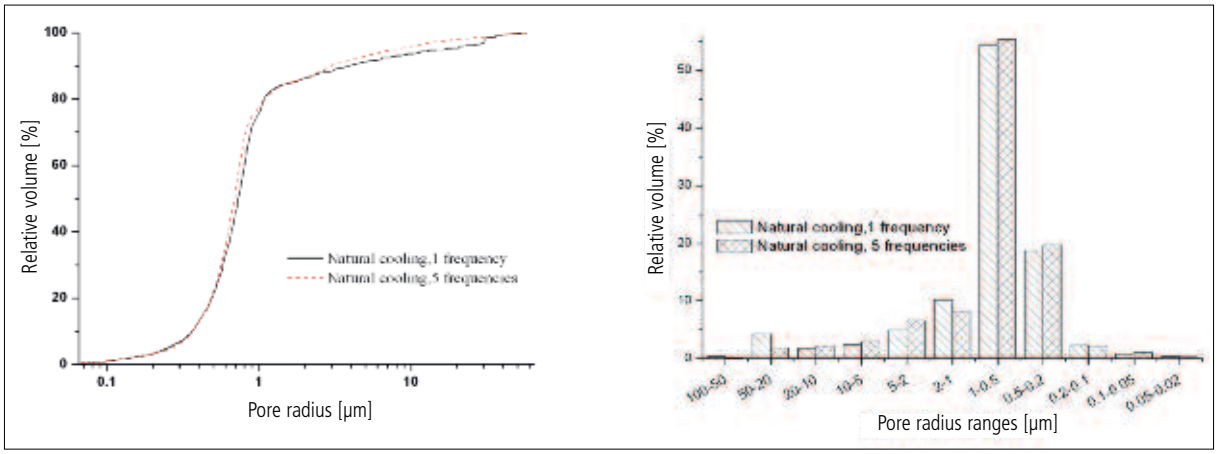


**Fig. 3** Pore size distribution of samples treated by heating-natural air cooling method

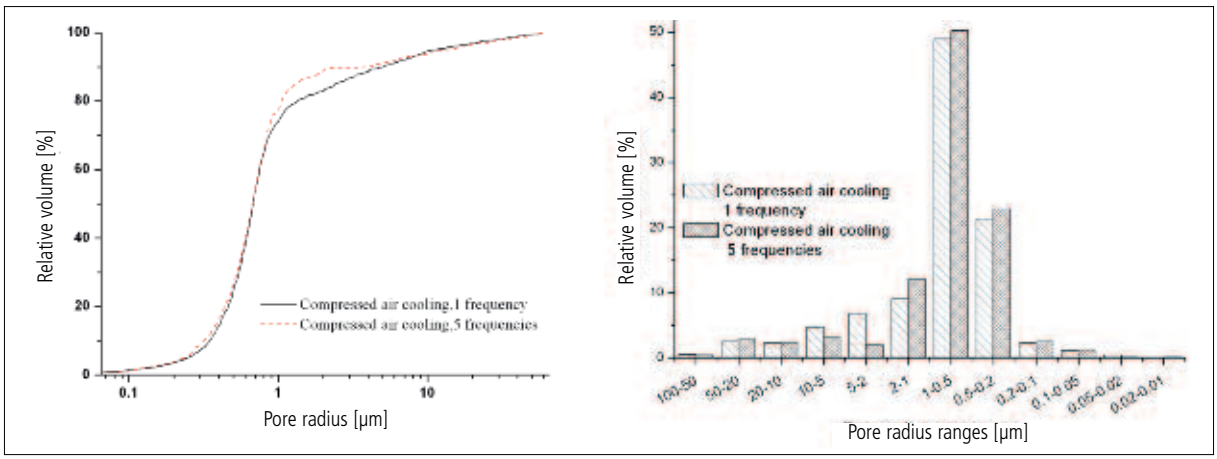


**Fig. 4** Pore size distribution of samples treated by heating-compressed air cooling method

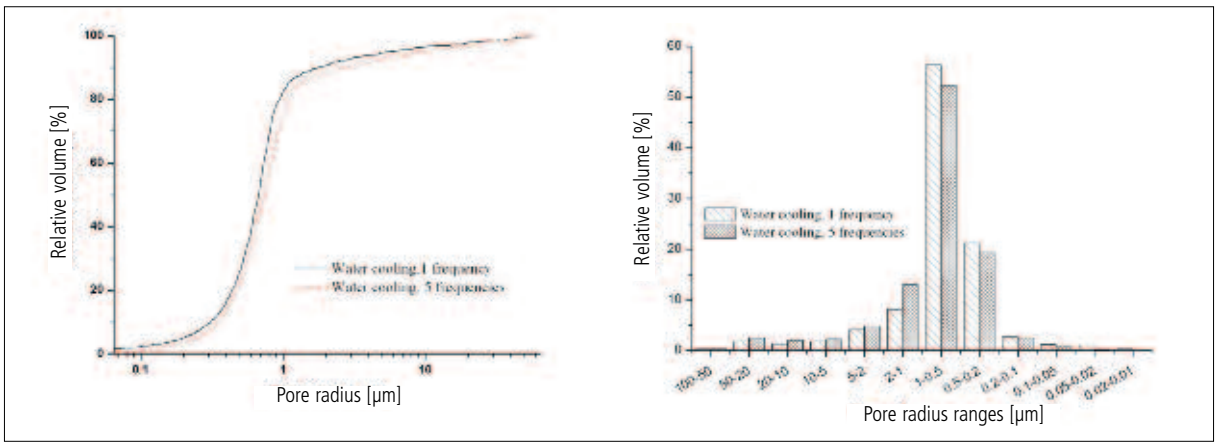


**Fig. 5** Pore size distribution of samples treated by heating-water cooling method

Fig. 1 and Fig. 2 show the results of residual bending strength and residual Young's modulus among the samples under different testing methods. The values used in Fig. 1 and Fig. 2 are the mean value that was calculated among each group and the standard error of means are also showed in the drawings. The residual bending strength or residual Young's modulus of unquenched samples is 100 % in the figures.

Based on Fig. 1 the residual bending strength of samples quenched by natural cooling and compressed air cooling method decreased as a function of the thermal shock cycles. However, for water quench test the residual bending strength values of samples decreased greatly but changed slightly after followed thermal shock cycles. The residual Young's modulus of the samples is generally decreased as a function of the thermal shock cycles.

**Tab. 3** Apparent porosity of the samples after thermal shock test [%]

| Heating-natural Cooling (1 Frequency) | Heating-compressed Air Cooling (1 Frequency) | Heating-water Cooling (1 Frequency) |
|---|---|---|
| 17,5 | 18,4 | 18,4 |
| **Heating-natural Cooling (5 Frequencies)** | **Heating-compressed Air Cooling (5 Frequencies)** | **Heating-water Cooling (5 Frequencies)** |
| 17,4 | 18,1 | 18,7 |

Fig. 3–5 are comparing pore size distributions of samples shocked by different thermal shock testing cycles. According Fig. 3 the pore size distribution curves (left) are quiet similar between different thermal cycles. Fig. 4 shows the pore size distribution curves (left) are quiet similar between different thermal cycles but the relative volume of range 1 to 2 µm is larger after five thermal shock cycles. The pore size distribution curve (left) in Fig. 5 shows more larger pores exist in the sample after 5 thermal shock cycles and the percentage of micropores (less 1 µm) is decreased; but the percentage of the pores larger than 1 µm is increased. The porosity of the samples is listed in Tab. 3.

Fig. 6 and Fig. 7 present the SEM micrographs of the samples. Cracks formed in the samples after one as well as five thermal shock cycles can be identified. According to Fig. 8 of SEM micrographs of the unquenched samples (treated under 1600 °C for 3 h), it can be seen that some cracks already existed in the original samples (left side).

Further investigations on the cracks of quenched samples are presented in Fig. 9. The sintering bonds among the particles of the samples shocked by natural cooling and compressed air cooling did not suffered. In contradiction, the sintering bonds between the particles of the samples shocked by water cooling were broken (circles in micrograph c).

For the samples shocked due to natural cooling, the temperature decreased slowly and the temperature difference in the sample is not critical during the cooling procedure. For the samples shocked due to compressed air

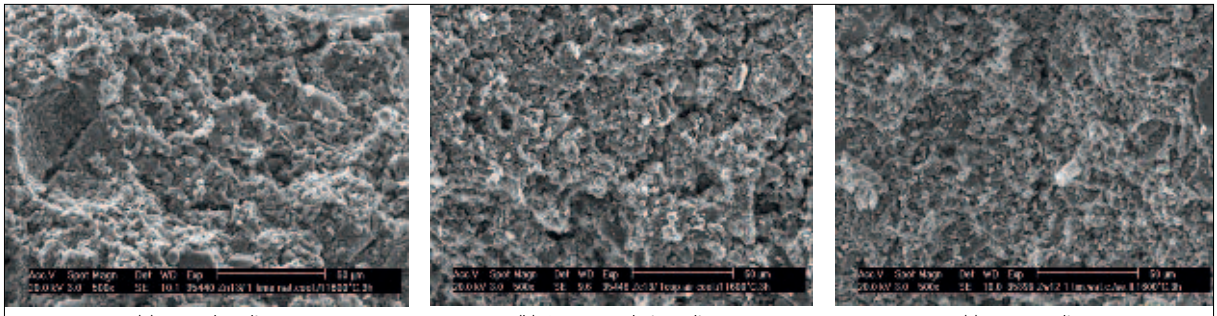

(a) Natural cooling (b) Compressed air cooling (c) Water cooling

**Fig. 6** SEM micrographs of samples suffered one frequency thermal shock

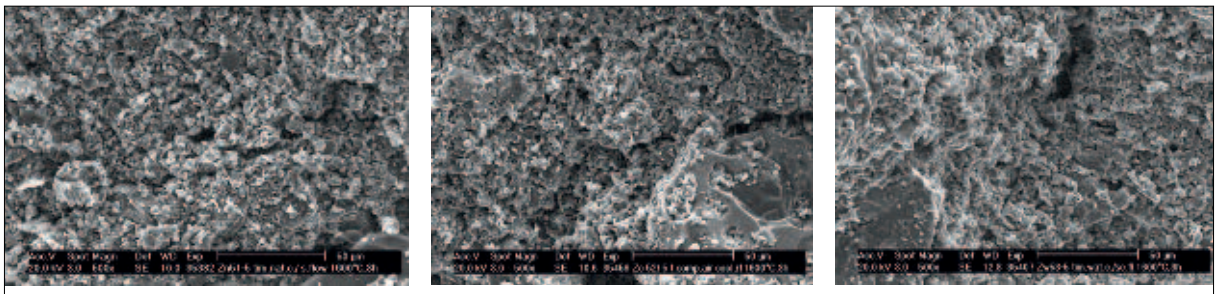

(a) Natural cooling (b) Compressed air cooling (c) Water cooling

**Fig. 7** SEM micrographs of samples suffered five frequencies thermal shock

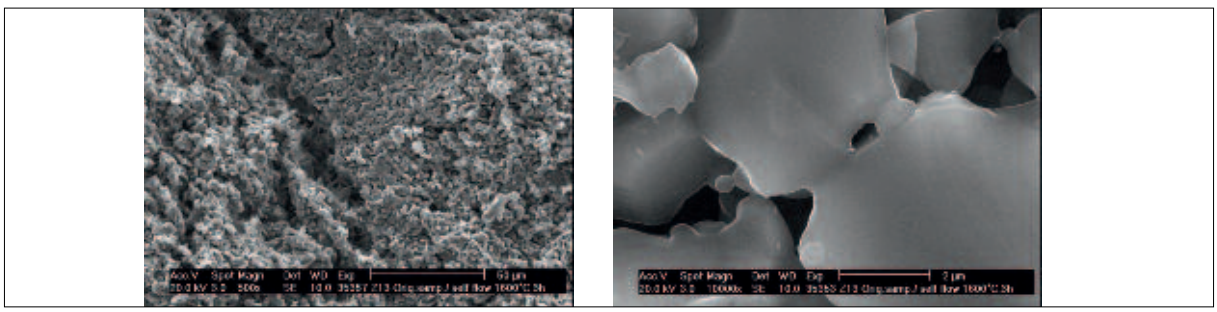

**Fig. 8** SEM micrographs of the unquenched sample

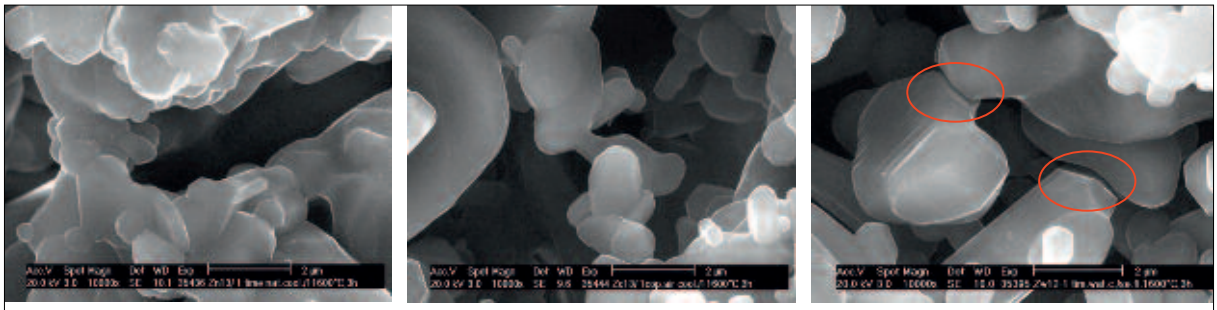

(a) Natural cooling (b) Compressed air cooling (c) Water cooling

**Fig. 9** SEM micrographs of samples shocked one frequency

cooling, the temperature on the surface is not reaching the room temperature also after 5 min air blowing, and the surface of the sample is still remaining enough hot; cracks might be formed only around the surface area and the temperature difference inner the samples is not high. In contradiction, according to Fig. 9c the thermal stresses caused by the water shock exceeds the strength of the sample and rapture of the sintering bond is registered.

Fig. 10 and Fig. 11 present the computerized tomography photos of the samples. There are not too much difference between one frequency shock and five frequencies shock cycles due to the natural cooling method. For the samples shocked due to compressed air quench method, more cracks are formed especially after five thermal shock cycles. The cracks are interconnected and a micro crack net work is generated. In contradiction for the samples shocked due to water quench testing method, the cracks did not present any kind of interconnection; critical big cracks pass through the section area. The apparent porosity of the samples shocked 1 cycle and 5 cycles under different testing method is changed a little (Tab. 3), while it can be seen from the Fig. 3 to Fig. 5 that the difference does existed in pore size distribution which might contribute to the bending strength and Young's modulus of the samples.

For samples suffered by heating-natural air cooling and heating-compressed air cooling, the relative volume of pores with diameter of 1–0,5 µm and 0,5–0,2 µm shocked 5 cycles is more than that shocked 1 cycle. But for samples suffered by water quench method, the relative volume of pores with

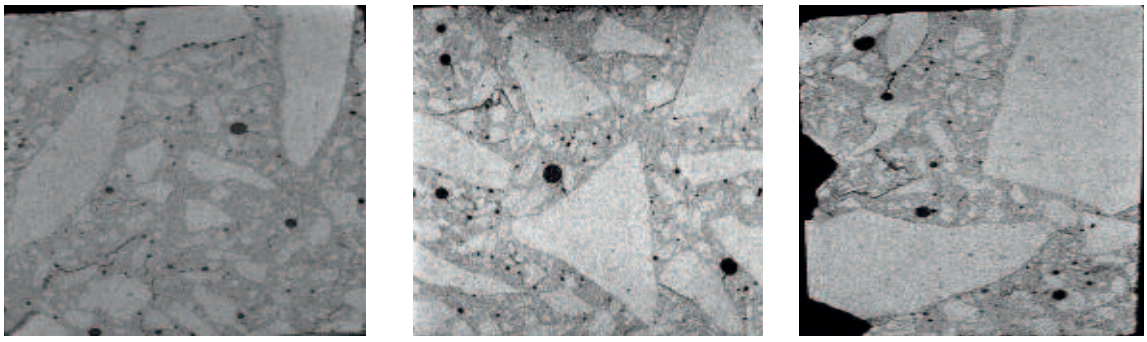

(a) Natural cooling (b) Compressed air cooling (c) Water cooling

**Fig. 10** 2D-computer tomography pictures of samples shocked one frequency

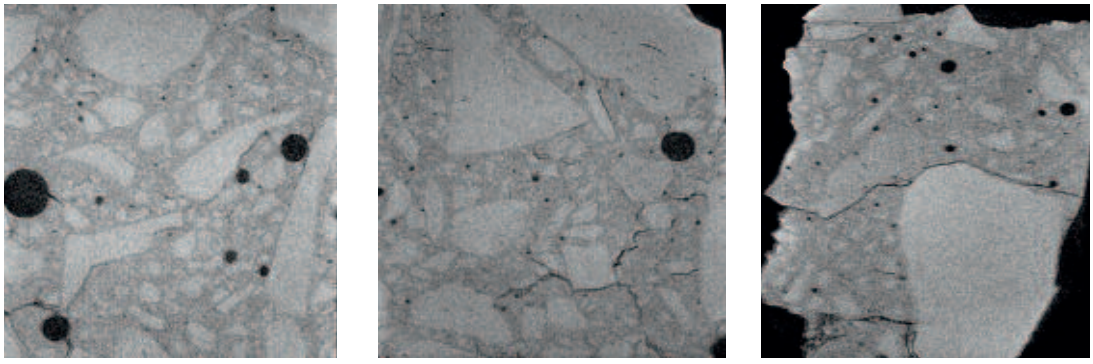

(a) Natural cooling (b) Compressed air cooling (c) Water cooling

**Fig. 11** 2D-computer tomography pictures of samples shocked 5 frequencies

diameter of 1–0,5 µm and 0,5–0,2 µm shocked 5 cycles is less than that shocked 1 cycle. It is also can be seen from the Fig. 9 to Fig. 11 that sample suffered by water quench is damaged seriously and is not suitable to simulate the condition in practice.

## 4 Conclusions

- The gradient of the registered residual Young's modulus and bending strength due to air cooling testing method and due to natural cooling method are similar.
- With the increased thermal shock cycles, the residual Young's modulus of all the samples is decreased; the residual bending strength is also decreased. The residual bending strength of the samples treated by water cooling is very small, and changed in a narrow range as a function of thermal shock cycles.
- Heating-air cooling testing method is better than heating – water quench method in the evaluation on thermal shock resistance of self-flow alumina castable samples according to this study.

## References


[1] Boccaccini, D.N.; et al.: Determination of thermal shock resistance in refractory materials by ultrasonic pulse velocity measurement. J. of Europ. Ceram. Soc. **27** (2007) 1859–1863

[2] Damhofa, F.; et al.: Experimental analysis of the evolution of thermal shock damage using transit time measurement of ultrasonic waves. J. of the Europ. Ceram. Soc. **29** (2009) 1309–1322

[3] Zhongqiu, Li; et al.: Microstructure, mechanical properties and thermal shock resistance of $ZrO_2$-$LaPO_4$ composites. J. of Alloys and Compounds 480 (2009) 863–866

[4] Xinghong Zhang; et al.: Modification and validation of the thermal shock parameter for ceramic matrix composites under water quenching condition. Mater. and Design **30** (2009) 4552–4556

[5] Posarac, M.; et al.: The ultrasonic and image analysis method for non-destructive quantification of the thermal shock damage in refractory specimens. Mater. and Design **30** (2009) 3338–3343

[6] Marenovic, S.; et al.: Thermal shock damage characterization of refractory composites. Ceram. Int. **34** (2008) 1925–1929

[7] Akiyama, S.; et al.: Thermal shock strength of $Al_2O_3$ by laser irradiation method. Ceram. Int. **27** (2001) 171–177

[8] Aksel, C.; Warren, P.D.: Thermal shock parameters [R, R''' and R''''] of magnesia-spinel composites. J. of the Europ. Ceram. Soc. **23** (2003) 301–308

[9] Pettersson, P.; et al.: Parameters for measuring the thermal shock of ceramic materials with an indentation-quench method. J. of the Europ.. Ceram. S. **22** (2002) 1883–1889

[10] Collin, M.; Rowcliffe, D.: Analysis and prediction of thermal shock in brittle materials. Acta Mater. **48** (2000) 1655–1665

[11] Posarac, M.; Dimitrijevic, M.: Determination of thermal shock resistance of silicon carbide/cordierite composite material using nondestructive test methods. J. of the Europ. Ceram. Soc. **28** (2008) 1275–1278

[12] Absi, J.; Glandus., J.C.: Improved method for severe thermal shocks testing of ceramics by water quenching. J. of the Europ. Ceram. Soc. **24** (2004) 2835–2838

[13] Volkov-Husović, T.D.; Jančić, R.M.: Thermal shock behavior of alumina based refractories: fracture resistance parameters and water quench test. Mater. Letters **38** (1999) 372–378

[14] Schmitt, N.; Burr, A.: Micromechanics applied to the thermal shock behavior of refractory ceramics. Mechanics of Mater. **34** (2002) 725–747

[15] Zhaoyou, C.: Prediction and evaluation on thermal shock resistance of refractories. Refractories (Chinese) **22** (1987) 50

[16] Hubálková, J.; Silva, W.M.; Aneziris, C.G.: X-Ray computed tomography as a tool for investigation of refractories. Proc. of 53rd Int. Coll. on Refractories 2010, Aachen, Germany, 49–52